Post-test analysis of a high-velocity steam condensation experiment with the system code TRACE

W. Jaeger[1] and W. Hering[2]
[1]Karlsruhe Institute of Technology, Institute of Fusion and Reactor Technology,
Kaiserstraße 12, 76131 Karlsruhe, Germany,
[2]Karlsruhe Institute of Technology, Institute for Neutron Physics and Reactor Technology,
Hermann-von-Helmholtz-Platz 1, 76344 Eggenstein-Leopoldshafen, Germany,
wadim.jaeger@kit.edu, wolfgang.hering@kit.edu,

ABSTRACT

This paper contributes to the ongoing validation process of the best-estimate system code TRACE with respect to steam condensation. TRACE is the thermal hydraulic reference code of the U.S. NRC for the simulation of LWRs during normal operation, operational transients and accidents. Therefore, it is necessary to verify and validate the empirical models used in TRACE. The empirical model used for condensation is a compromise between falling films, as on containment structures, and sheared films, as during high-velocity flows in condensers. The validation of the condensation model is based on comparison of experimental data with TRACE predictions by means of post-test analysis. One of the open issues is to show the general applicability of such empirical models, especially at borderline boundary conditions like high-velocity steam flow. Up to now, the field of condensation with downward facing flow and high-velocity steam is still open field for validation due to the very limited number of available experimental data. To assess the predicting capabilities of TRACE during high-velocity steam condensation, a dedicated experiment is selected. This experiment, with its various test scenarios and steam velocities between 100 and 300 m/s, provides sufficient data to perform a post-test analysis. The comparison between experiment and TRACE caclulation is made based on the wall temperature, the coolant temperature, and the heat flux, each of them as function of the test section length. Due to the good qualitative and quantitative agreement between experiment and TRACE prediction it can be concluded that TRACE is applicable to represent high-velocity steam condensation.

1. Introduction to high-velocity steam condensation

This section will give a short overview on steam condensation in general and on the current physical treatment in the system code TRACE. Section 2 describes the test facility. The comparison of experimental results and calculation is given in section 3. The results will be discussed in section 4. A summary and an outlook are given in section 5.

The process of steam condensation takes place in every thermal power plant operating with a Clausius-Rankine cycle. During normal operation of a plant, water vapor is cooled down and condensed from gaseous state to liquid state in a condenser. During off-normal and accidental behaviour, vapor, e.g., is condensed on large surfaces like the containment of a nuclear power plant. Thereby, the condensation takes place when the surface temperature of the heat transfer structure is below the saturation temperature corresponding to the present vapor partial pressure.

TRACE is best estimate system code. Its main field of application is the thermal-hydraulic analysis of normal operation, operational transients and accidental conditions in light water reactors. Thereby, TRACE follows a 6-Equation, 2-Fluid approach. For each water phase, liquid and gas, the field equations for the conservation of mass, energy and momentum are solved. In order to close these field equations additional models are needed. These models provide information regarding, e.g., the heat transfer.

Due to the intended use of TRACE for the analysis of light water reactors, the physical models, including condensation, must be applicable for a wide range of boundary conditions. With respect to condensation, the TRACE models are applicable to falling films and to sheared films. Falling films are typical for condensation on a large surface, like in a containment. Sheared films appear during high-velocity flows inside condenser tubes. In TRACE, the primary mode of condensation is the filmwise condensation [1]. The film thickness is used as characteristic length. Hence, the heat transfer is defined as follows:

$$h = \mathrm{Nu}_{\mathrm{condensation}} \cdot \frac{k_{\mathrm{liquid}}}{\delta_{\mathrm{liquid}}}. \tag{1}$$

For the Nusselt number the quadratic power law is used to weight the laminar and turbulent parts of the heat transfer, see Eq. (2):

$$\mathrm{Nu}_{\mathrm{condensation}} = \sqrt{\left(\mathrm{Nu}_{\mathrm{laminar}}{}^{2} + \mathrm{Nu}_{\mathrm{turbulent}}{}^{2}\right)}. \tag{2}$$

For the laminar Nusselt number the model of Kuhn, Schock and Peterson [2] is used and adopted for interfacial heat transfer, writes as follows:

$$\mathrm{Nu}_{\mathrm{laminar}} = 2 \cdot (1 + 1.83 \cdot 10^{-4} \cdot \mathrm{Re}_{\mathrm{film}}). \tag{3}$$

The turbulent Nusselt number is based on the Gnielinski model [3] for turbulent pipe flow and the Filonenko model for the friction factor f [4]. To allow an application for liquid films, the Gnielinski correlation is divided by four [1]:

$$\mathrm{Nu}_{\mathrm{turbulent}} = \frac{1}{4} \cdot \frac{\frac{f}{2} \cdot (\mathrm{Re}_{\mathrm{film}} - 1000) \cdot \mathrm{Pr}_{\mathrm{film}}}{1 + 12.7 \cdot \sqrt{\frac{f}{2}} \cdot \left(\mathrm{Pr}_{\mathrm{film}}^{\frac{2}{5}} - 1\right)} \tag{4}$$

with

$$f = [1.58 \cdot \ln(\mathrm{Re}) - 3.28]^{-2}. \tag{5}$$

The Reynolds and Prandtl number for the film, as used in the correlations above, are defined as follows:

$$\mathrm{Re}_{\mathrm{film}} = 4 \cdot \frac{\Gamma_{\mathrm{film}}}{\eta_{\mathrm{liquid}}}, \tag{6}$$

$$\mathrm{Pr}_{\mathrm{film}} = \frac{\eta_{\mathrm{liquid}} \cdot c_{p,\mathrm{liquid}}}{k_{\mathrm{liquid}}}. \tag{7}$$

Both, the laminar and turbulent Nusselt number models are validated against a variety of experimental and numerical data by the TRACE developers. The used empirical models are well able to represent the chosen experiment. Hence, it is expected that the experimental results used in this study are reproducible with the condensation modelling approach of TRACE.

2. Description of the experimental facility

The experiment considered in this investigation dates back to 1967. Local heat transfer coefficients and static pressures for condensation of high-velocity steam within a tube were measured. The experiments were performed in a NASA facility in the Lewis Research Center [5]. The intention of the experiment was to demonstrate the applicability of Rankine-cycles for space-power systems. At high steam velocities the Froude number becomes large and is comparable to zero gravity systems.

This experiment is selected, because it offers a wide range of parameter combination (pressure, steam velocities, etc.). Furthermore, the simple tube-in-tube design of the test section can easily be modelled with best estimate system codes like TRACE. The facility and the test section are shown in Figure 1 and Figure 2, respectively. Figure 1 shows the two loop test facility. The left side in Figure 1 shows the vapor system, while the right side of Figure 1 shows the coolant system. In both cases water is used as fluid. The separation of the two loops is realised by the tube-in-tube test condenser. This test condenser (Figure 2) is a coaxial shell and tube heat exchanger in vertical direction. The high-velocity steam enters the central pipe at the top and flows downward, while condensing. The coolant water enters the outer tube at the bottom and flows upward, while heating up.

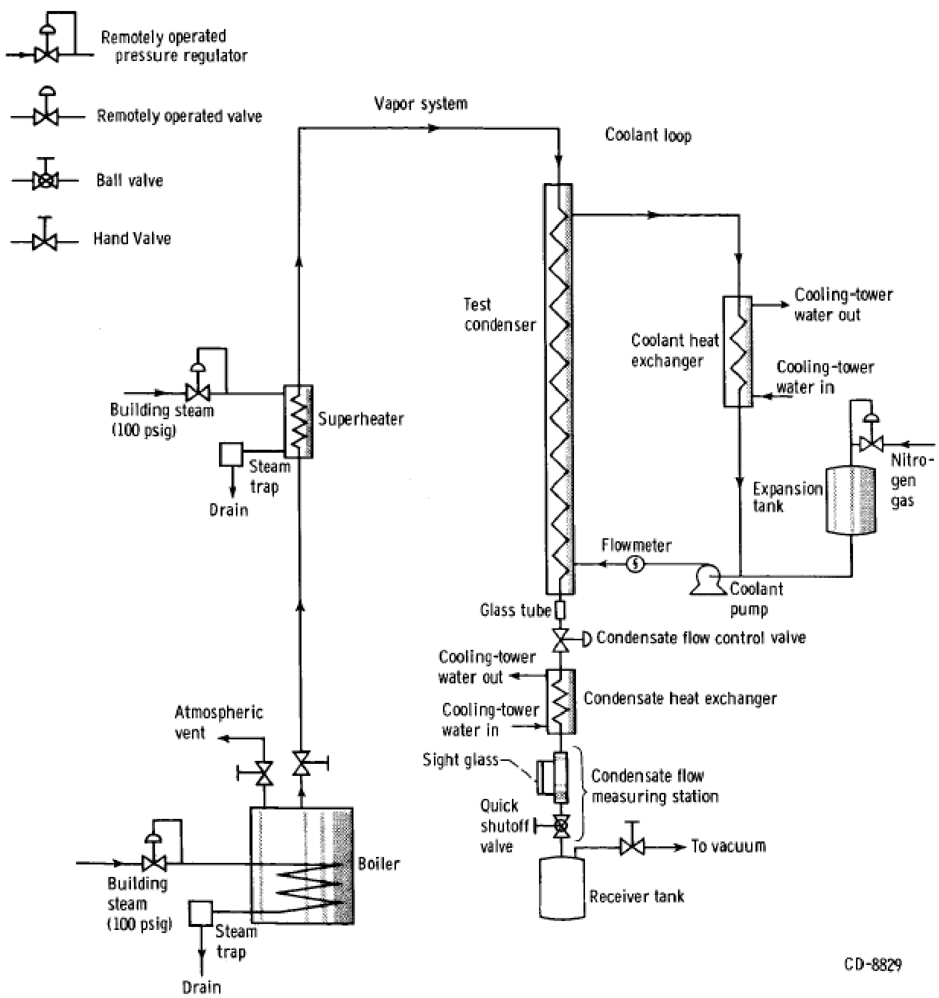

Figure 1 Schematic drawing of the test facility [5]

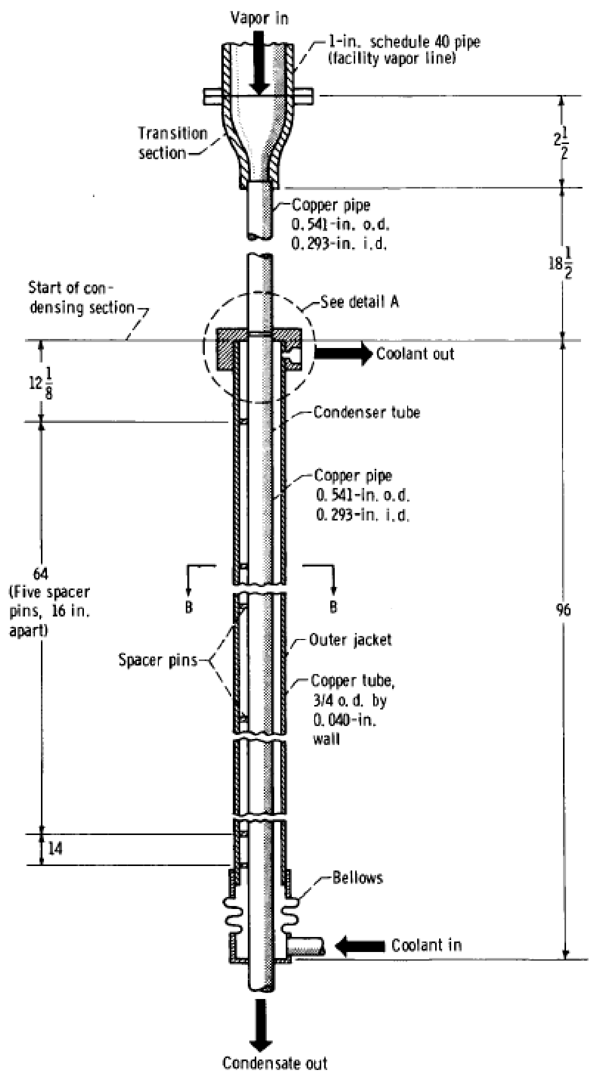

Figure 2 Tube-in-tube test section (dimensions in inch) [5]

The main geometrical data are collected in Table 1, while the main operational parameters are listed in Table 2.

Table 1 Main geometrical parameters and their dimensions

Parameters [Unit]	**Dimension**
Inner tube inner diameter [mm]	7.44
Inner tube outer diameter [mm]	13.74
Outer tube inner diameter [mm]	17.02
Outer tube outer diameter [mm]	19.05
Test condenser length [mm]	2438

Table 2 Main operational parameters and their range

Parameters [Unit]	Parameter range
Vapor flow rate [kg/s]	0.0038 … 0.0199
Vapor inlet pressure [bar]	1.03 … 2.70
Vapor inlet temperature [K]	386 … 417
Vapor inlet velocity [m/s]	95 … 310
Vapor inlet quality [%]	> 99
Condensing length [m]	0.33 … 2.04
Coolant flow rate [kg/s]	0.0510 … 0.2747
Coolant inlet temperature [K]	289 … 310
Coolant outlet temperature [K]	308 … 370

The test condenser is modelled with TRACE. Thereby, the inner and outer tube are modelled as separate TRACE pipe components with independent input and boundary conditions. The hydraulic diameter and the flow area for each tube are calculated and imposed on the TRACE pipe component to represent a tube (inner tube) and an annulus (outer tube). For each tube the pressure boundary is defined at the outlet. The inlet temperature and flow rate of the steam and the coolant are defined at the tube inlet. To account for the tube-in-tube character of the test condenser, the two tubes are connected by a heat structure. This heat structure has the characteristic of the inner tube wall (thickness, material, etc.). Each of the modelled TRACE pipes consists of 240 cells, each of them 10 mm long.

3. Comparison of experimental results and TRACE calculations

In total, 58 combinations of steam flow rate, steam inlet temperature, steam inlet pressure, coolant flow rate and coolant inlet temperature are investigated. These 58 combinations are listed below in Table 3.

Table 3 Test runs and their parameter combinations

Test run	Steam flow rate [kg/s]	Coolant flow rate [kg/s]	Steam temp. [K]	Coolant temp. [K]	Steam pressure [Pa]
163	7.5599E-03	1.0458E-01	390.93	297.04	1.1680E+05
164	5.7077E-03	6.9929E-02	388.71	295.37	1.4438E+05
165	5.5817E-03	1.0458E-01	388.15	297.04	1.5106E+05
166	5.3927E-03	1.3381E-01	389.26	299.26	1.5224E+05
167	7.6607E-03	6.7409E-02	396.48	293.71	1.6251E+05
168	7.2827E-03	1.0647E-01	395.37	298.71	1.5803E+05
169	7.3709E-03	1.3167E-01	396.48	299.82	1.6478E+05
170	7.1441E-03	1.6695E-01	396.48	301.48	1.6740E+05
171	8.6183E-03	6.6779E-02	398.15	293.71	1.8492E+05
172	8.4923E-03	1.1088E-01	398.15	297.04	1.8209E+05
173	8.5049E-03	1.3230E-01	398.15	299.82	1.8312E+05
174	8.5931E-03	1.6758E-01	398.15	301.48	1.8085E+05

Test run	Steam flow rate [kg/s]	Coolant flow rate [kg/s]	Steam temp. [K]	Coolant temp. [K]	Steam pressure [Pa]
175	6.1487E-03	5.1029E-02	389.82	291.48	1.2955E+05
176	7.4717E-03	1.0143E-01	392.04	293.71	1.0363E+05
177	1.0080E-02	1.3419E-01	400.93	305.93	1.4982E+05
178	1.1516E-02	1.3419E-01	402.59	294.82	1.7623E+05
179	1.2461E-02	1.3419E-01	404.82	307.04	2.0291E+05
181	1.3356E-02	1.9882E-01	404.26	302.04	1.7754E+05
185	1.6506E-02	2.6208E-01	411.48	303.71	2.2056E+05
187	1.3331E-02	1.7640E-01	404.82	302.04	1.9064E+05
188	1.4729E-02	1.7640E-01	410.37	303.15	2.4601E+05
191	1.3734E-02	2.7468E-01	405.37	308.15	1.7857E+05
196	8.3159E-03	2.3234E-01	392.59	301.48	1.3252E+05
197	9.1097E-03	2.3234E-01	398.71	302.04	1.6547E+05
198	9.8278E-03	2.3234E-01	399.26	302.59	1.5465E+05
199	1.0143E-02	2.3234E-01	399.82	302.59	1.5037E+05
200	1.0584E-02	2.3234E-01	400.37	303.15	1.3865E+05
205	1.3268E-02	2.4343E-01	404.26	304.26	2.5986E+05
206	7.9883E-03	1.5750E-01	398.15	300.37	1.9119E+05
207	9.6010E-03	2.1798E-01	399.26	302.59	1.6968E+05
208	1.0143E-02	2.1798E-01	399.82	303.71	1.6085E+05
209	1.0848E-02	2.1798E-01	400.37	303.15	1.4569E+05
212	5.7329E-03	8.2529E-02	389.82	296.48	1.4348E+05
213	6.4889E-03	8.2529E-02	390.37	295.93	1.3403E+05
215	7.1063E-03	1.0458E-01	389.82	295.93	1.2486E+05
216	7.3331E-03	1.0458E-01	390.37	295.93	1.2397E+05
217	7.5599E-03	1.0458E-01	390.93	295.93	1.1845E+05
219	3.8429E-03	2.0689E-01	388.15	297.04	1.6141E+05
220	5.1533E-03	2.0689E-01	392.59	298.71	1.5079E+05
221	5.6699E-03	2.0689E-01	394.82	299.26	1.4534E+05
222	6.7913E-03	2.0689E-01	396.48	300.37	1.2914E+05
223	7.7363E-03	2.0689E-01	397.59	300.93	1.1156E+05
224	9.3995E-03	2.0689E-01	400.93	302.04	1.6692E+05
225	6.9677E-03	2.1735E-01	398.71	302.04	2.0746E+05
226	5.6699E-03	2.2743E-01	388.15	302.04	1.3838E+05
227	7.7111E-03	2.2743E-01	393.71	303.71	1.4293E+05
228	8.5553E-03	2.2743E-01	396.48	304.26	1.7975E+05
229	9.1349E-03	2.2743E-01	400.37	304.82	2.1098E+05
233	1.3205E-02	2.3234E-01	404.26	307.04	1.8802E+05
234	1.3381E-02	2.2780E-01	403.71	308.15	1.8478E+05
235	1.5347E-02	2.2780E-01	408.71	310.37	2.3959E+05
236	1.6128E-02	2.2780E-01	408.71	310.37	2.2904E+05
237	1.0508E-02	1.1970E-01	398.15	300.37	1.8299E+05
238	1.1403E-02	1.1970E-01	403.71	300.93	2.2629E+05
239	4.1453E-03	1.0458E-01	385.93	289.26	1.5348E+05

Test run	Steam flow rate [kg/s]	Coolant flow rate [kg/s]	Steam temp. [K]	Coolant temp. [K]	Steam pressure [Pa]
240	1.6443E-02	2.3373E-01	409.26	305.93	2.3015E+05
241	1.8522E-02	2.3373E-01	413.71	307.04	2.7124E+05

All these test runs are modelled with TRACE. Selected results will be presented in this section and discussed in the next section. The results of the TRACE calculations will be compared to the experimental data. Due to the limited number of available data only a few parameters are shown for comparison. The first parameter to be considered is the wall temperature on the inside of the inner tube, meaning the surface, which is in contact with the condensing high-velocity steam. The second parameter available for comparison is the coolant temperature heat-up, meaning the water temperature development inside the outer tube. Both values are plotted as a function of the axial length. On the left side of Figure 3 and Figure 4 the experimental data for six test runs are compared to the TRACE calculations. Thereby, the coolant enters from the bottom of the test condenser in the outer tube. This corresponds to an axial length of 2.42 m in the following two figures. This comparison shows a good agreement for most of the test runs. The agreement of the calculated coolant temperatures with the experimental results is even very good. For the wall temperature, small discrepancies are shown. From the six cases, only for one case (test run 176) no agreement is given. In fact, out of the 58 test runs several cases cannot be reproduced with TRACE. An explanation is given in the next section.

The third parameter to compare is the heat flux on the inside surface of the inner tube. The comparison of experimental results and TRACE calculations is given on the right side of Figure 3 and Figure 4. Again, the qualitative assessment can be considered successful with the exception of test run 176. Besides the matching values of temperatures and heat fluxes, the trend lines indicate also the condensing length. From a practical point of view, the condensation length is the part of the test condenser where a large temperature difference between the wall and the coolant exists. As an example for length of the condensing zone, test run 163 (top graphs of Figure 3) is chosen. The wall temperature decreases almost linearly with a rather flat tendency and eventually drops quickly at an axial length of 1.0 to 1.25 m. At 1.5 m the wall temperature and the coolant temperature are almost identical indicating that no heat is transferred from the inner to the outer tube. This is confirmed by the heat flux plots. In there, a rather constant heat flux is present for the first meter. Within a short section, 1.0 to 1.3 m, the heat flux drops down.

Due to the different input and boundary conditions, like the steam flow rate and the steam temperature on the one side and the coolant flow rate coolant temperature on the other side, different condensing lengths will be established.

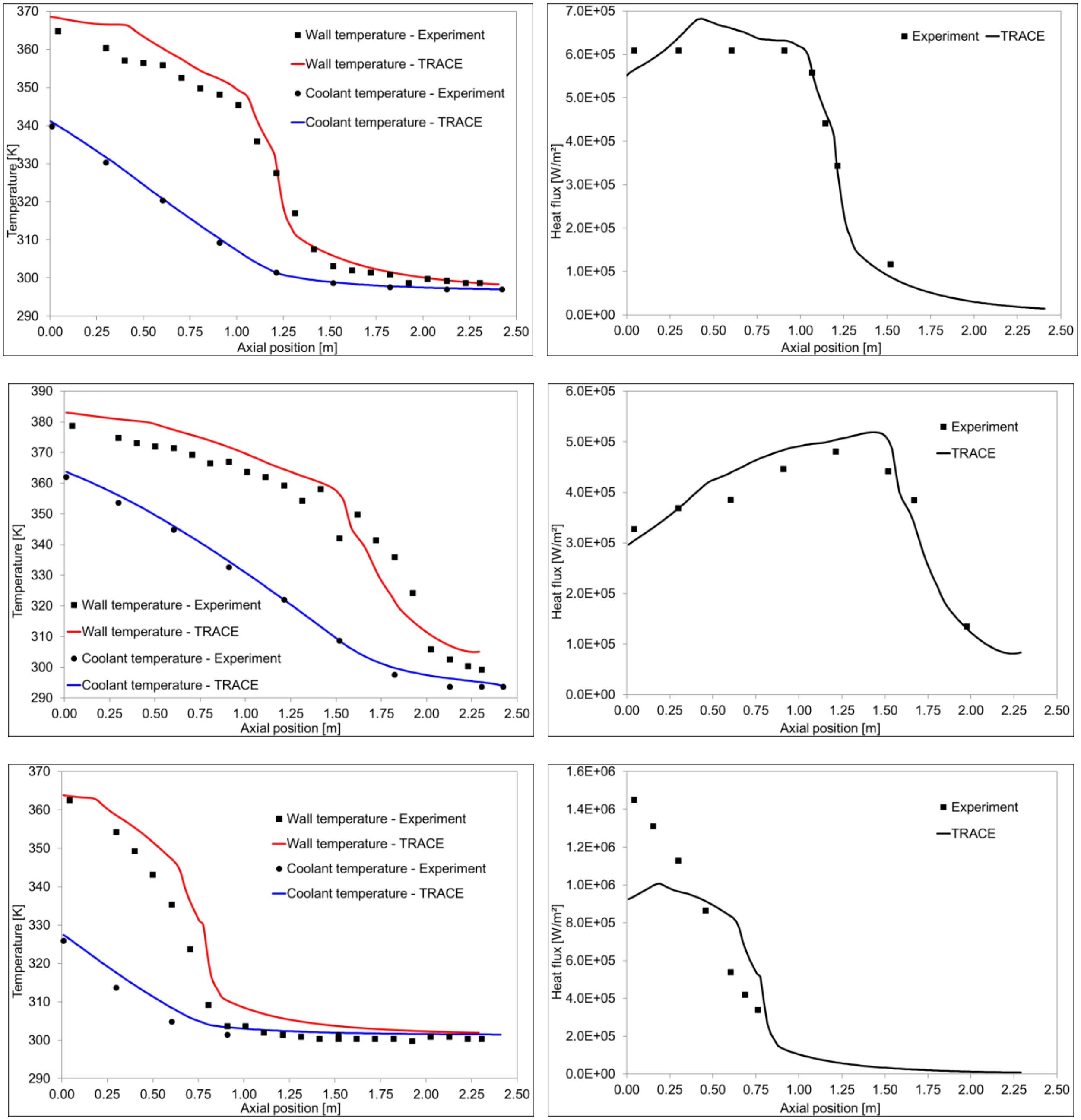

Figure 3 Experimental data (symbols) in comparison to TRACE calculations (lines) for the inner wall temperature of the inner tube, the coolant temperature (both on the left diagrams) and the heat flux from the inner tube to the outer tube (on the right diagrams) as a function of the axial length for test runs 163 (top), 167 (center) and 170 (bottom)

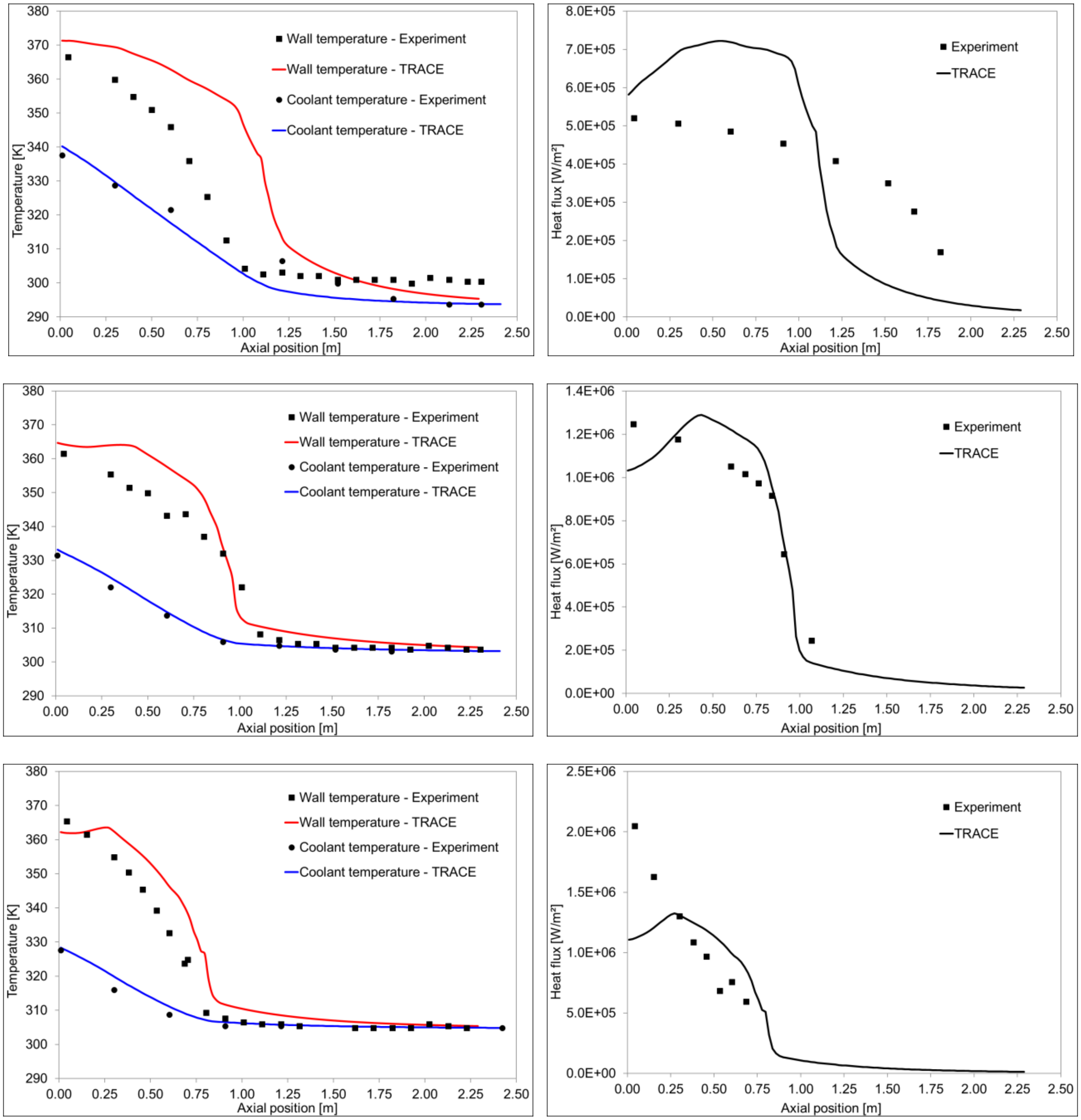

Figure 4 Experimental data (symbols) in comparison to TRACE calculations (lines) for the inner wall temperature of the inner tube, the coolant temperature (both on the left diagrams) and the heat flux from the inner tube to the outer tube (on the right diagrams as a function of the axial length for test runs 176 (top), 209 (center) and 229 (bottom)

4. Discussion of the investigation

Based on the viewgraph norm or the qualitative assessment, most of the experimental test runs can be represented very well with TRACE. Taking into account the physical instabilities related to high-velocity steam condensation, the results of this validation procedure can be considered successful. Nevertheless, some test runs cannot be represented with the current TRACE version. The question which needs to be answered now is whether the problem is related to the experiment or to the calculation. With respect to the experiment it can be stated that some uncertainties exist, which might influence the outcome of this investigation. It is well known that every measurement is more or less affected by uncertainties. The challenge is to identify and quantify them.

One of the main differences between experiments and simulations is the treatment of input and boundary conditions. In simulations, the conditions are fixed, while in the experiments certain fluctuations must be considered. A mass flow rate in a simulation will be, say, 1 kg/s. In the experiment, an uncertainty of $|X| > 0$ is always present. The same must be considered for the inlet temperature and so on. Similar to the boundary conditions, the measured quantities of an experiment are affected by uncertainties. Temperature differences, e.g., can only be measured with a certain precision and accuracy. In the present case, the temperature difference needed to calculate the local condensation heat transfer coefficient is only a few Kelvin. A deviation of, say, 1 K between experiment and simulation will cause rather large differences on the heat transfer coefficient. Differences of more than 50 % are possible. Other quantities affected with uncertainties are: the pressure (and therefore the saturation temperature), the mass flow rate, etc.

Unfortunately, no test run specific uncertainties related to the temperature or mass flow rate measurements are given. Within the documentation of the experiment, the temperature error is calculated to be in general less than 1 K. It remains to be clarified if the consideration of (small) measurement uncertainties in the TRACE calculations will result in a successful comparison of the experimental data and calculations for test run 176. Nevertheless, it would be interesting to perform an uncertainty and sensitivity study to identify the influences of input and boundary condition uncertainties on the results.

The only information regarding experimental uncertainties provided within the original document are related to test run specific heat balance errors. These heat balance errors were calculated by *"… taking the difference between the heat gained by the coolant and the total heat rejected by the test fluid and dividing by the heat gain of the coolant*" [5]. These heat balance errors range from +7 % to – 9.5 %. The analysis of the experiment reveals that the heat balance error is related to the coolant flow rate, as indicated in Figure 5.

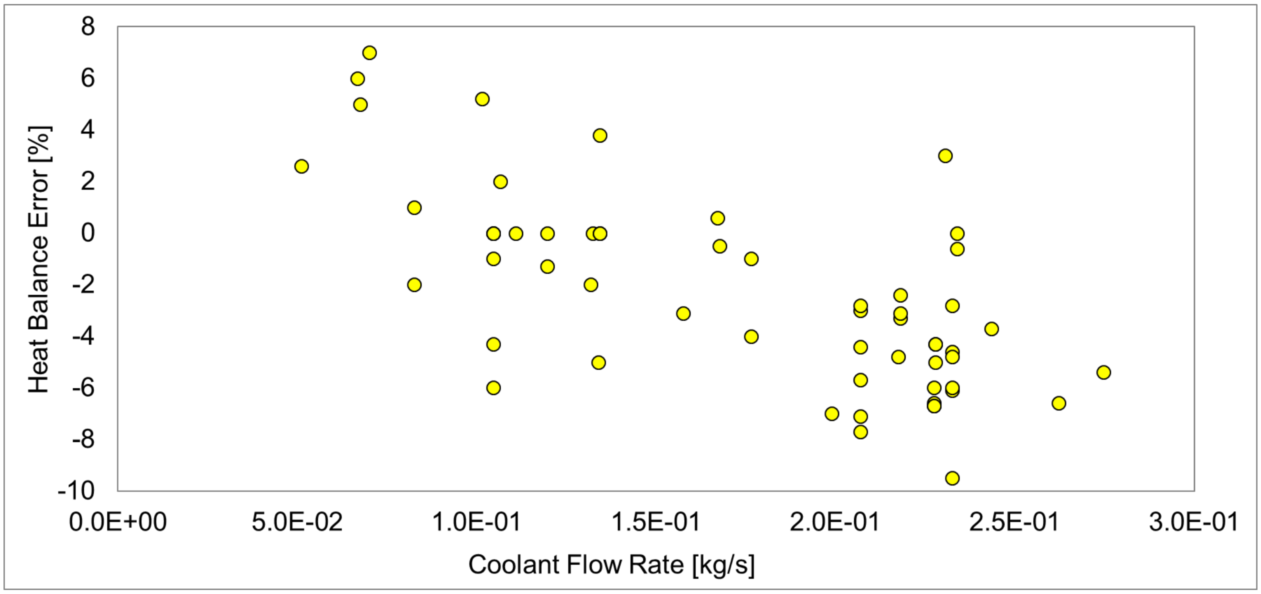

Figure 5 Heat balance error as a function of the coolant mass flow rate for all 58 test runs

In the context of discussing the results, the comparison with other best estimate system codes will be briefly evaluated. For this purpose, results are taken from simulations performed with the commercial tool APROS [6, 7]. APROS is also a 6-Equation model with empirical models for the closure of the conservation equation [8]. As an example, the wall temperature for test run 163 is used for the sake of comparison, see Figure 6. It is visible that the trends for the two code calculations and the experiment are identical; especially the condensing length is calculated very well. The main differences between the codes are the wall temperatures at the lower position, meaning close to the steam inlet. APROS slightly under-predicts the wall temperatures, while TRACE is slightly over-predicting the wall temperature. The differences might be caused by different empirical models for the condensation heat transfer in TRACE and APROS. In order to identify the reasons for this behaviour a future investigation should be performed to compare the modelling approaches between different best estimate system codes in detail. Nevertheless, the comparison shows that system codes in general are well able to represent such complex experiments.

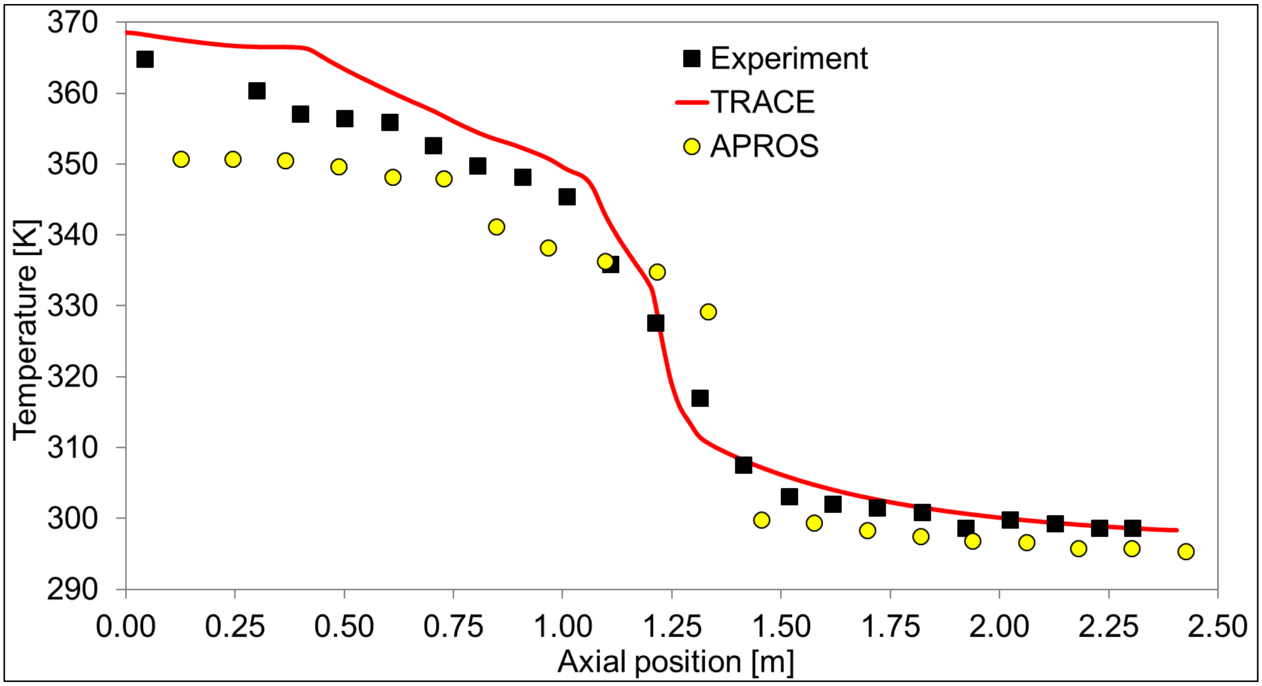

Figure 6 Wall temperature as a function of the axial length for test run 163 - Comparison of experimental results and calculations with TRACE and APROS

5. Summary and outlook

Experimental data for high-velocity steam condensation is compared to TRACE calculations. In total 58 experimental test runs are modelled and evaluated. Most of these rest runs can be represented (very) well with TRACE. The deviations between experiment and calculation are low, from an engineering perspective. It can be concluded that the empirical models for high-velocity steam condensation and their implementation into the TRACE code is successful.

The following steps will be considered for further studies:

- Application of different empirical models for the condensation heat transfer, in particular for different Nusselt number models.
- Comparison of different best estimate system codes with respect to their (condensation) heat transfer approach.
- Uncertainty and sensitivity study to identify the input and boundary conditions with the highest influence on the output. Quantification of these influences.
- Simulation of other high-velocity steam condensation experiments.

6. Nomenclature

c_p	Specific heat capacity
h	Heat transfer coefficient
k	Thermal conductivity
δ	Film thickness
Γ	Film flow rate
η	Dynamic viscosity
Nu	Nusselt number
Pr	Prandtl number
Re	Reynolds number

7. References

[1] U.S. NRC, "TRACE V5.0 Theory manual," US NRC, Washington, D.C., 2012.

[2] S.Z. Kuhn, V.E. Schrock and P.F. Peterson, "Final Report on U. C. Berkeley Single Tube Condensation Studies," UCB-NE-4201, August 1994.

[3] V. Gnielinski, "New Equations flow regime Heat and Mass Transfer in Turbulent Pipe and Channel Flow," International Chemical Engineering, Vol. 16, 1976, pp. 359-368,

[4] G.K. Filonenko, "Hydraulic Resistance in Pipes," (in Russian), Teplonergetika, Vol. 1, 1954, pp. 40-44.

[5] J.H. Goodykoontz and R.G. Dorsch, "Local heat-transfer coefficients and static pressures for condensation of high-velocity steam within as tube", NASA Technical Note NASA TN D-3953, 1967.

[6] H. Herbell, A. Class, J. Starflinger and T. Schulenberg, "Design and Stability Limits of the HPLWR Reheater", Proceedings of the 2010 International Congress on Advances in Nuclear Power Plants, San Diego, Calif., USA, 2010 June 13.-17.

[7] H. Herbell, Thermohydraulische Auslegung des Zwischenüberhitzers eines High Performance Light Water Reactors (in German), PhD Thesis, Karslruhe Institute of Technology, 2011.

[8] M. Hänninen and J. Ylijoki "The Constitutive Equations of the APROS Six-Equation Model", VTT Finnland and Fortum, APROS Version 5.08, 2007.